Comparative study of anchoring groups for molecular electronics: structure and conductance of Au–S–Au and Au–NH$_2$–Au junctions

Comparative study of anchoring groups for molecular electronics: structure and conductance of Au–S–Au and Au–NH$_2$–Au junctions

I S Kristensen, D J Mowbray, K S Thygesen and K W Jacobsen

Center for Atomic-scale Materials Design (CAMD), Department of Physics, Building 307,
Technical University of Denmark, DK-2800 Kongens Lyngby, Denmark

Abstract
The electrical properties of single-molecule junctions, consisting of an organic molecule
coupled to metal electrodes, are sensitive to the detailed atomic structure of the molecule–metal
contact. This, in turn, is determined by the anchoring group linking the molecule to the metal.
With the aim of identifying and comparing the intrinsic properties of two commonly used
anchoring groups, namely thiol and amine groups, we have calculated the atomic structure and
conductance traces of different Au–S–Au and Au–NH$_2$–Au nanojunctions using density
functional theory (DFT). Whereas NH$_2$ shows a strong structural selectivity towards atop-gold
configurations, S shows large variability in its bonding geometries. As a result, the conductance
of the Au–NH$_2$–Au junction is less sensitive to the structure of the gold contacts than the
Au–S–Au junction. These findings support recent experiments which show that amine-bonded
molecules exhibit more well-defined conductance properties than do thiol-bonded molecules.

(Some figures in this article are in colour only in the electronic version)

1. Introduction

A detailed, quantitative understanding of the electron transport
properties of molecular junctions composed of a single
molecule between two metallic electrodes is an essential step
for the development of molecular electronics. Experiments on
single-molecule junctions often suffer from a large variability
in the measured conductance, probably originating from details
beyond experimental control. In the case of molecules linked to
metal electrodes via a sulfur atom, that is, through thiol linking
groups, the conductance shows a strong junction to junction
variation within the same experiment [1], as well as between
different sets of experiments [2–5]. More recent experimental
and theoretical works suggest that the use of amine (NH$_2$)
anchoring groups yields junctions with a more well-defined
conductance [6].

Knowledge about the atomistic contact geometry must be
obtained through detailed comparisons between experimental
and theoretical results. For certain types of systems,
calculations based on density functional theory (DFT) agree

well with experiments and yield valuable insights. Such
systems include atomic wires [7, 8] and metal contacts with
small chemisorbed molecules [9, 10]. Even though these types
of systems are not directly relevant for molecular electronics,
they are important for developing our understanding of electron
transport at the nanoscale, and as such they can be considered
as simple benchmark systems. For larger and more complex
molecular junctions, such as benzene-dithiolate, rather large
disagreements have been observed, both between individual
experimental results and in comparison with theory [6, 11, 12].

In this paper, we compare the transport properties of
the thiol and amine anchoring groups by performing DFT
calculations for both structure and conductance of Au–S–Au
and Au–NH$_2$–Au nanojunctions. In the case of sulfur we
consider two different geometries: a top–top configuration
where the sulfur atom is bonded to a single gold atom on each
side, and a top–hollow configuration where sulfur is bonded
to a single gold atom on one side and three gold atoms on
the other side. We simulate a break junction experiment by
calculating the conductance as the contact is pulled apart, and

we find a strong dependence on the local atomic structure. In contrast to sulfur, we find that the amine group always binds to a single Au atom on each side of the junction. We consider two junction geometries: a symmetric top–top configuration similar to the one found for S, and an asymmetric top–top configuration. The pronounced structural selectivity of the amine group leads to very similar conductance traces for the two configurations.

2. Method

The DFT calculations have been performed using the plane-wave-based pseudopotential code DACAPO [13][1]. The molecular contacts are described in a supercell containing the sulfur atom or amine group sandwiched between two four-atom Au pyramids attached to Au(111) surfaces. We include six Au atomic layers each containing 3×3 atoms in the surface plane. Periodic boundary conditions are imposed in all directions. We use a 4×4 Monkhorst–Pack grid to sample the Brillouin zone in the surface plane both for the total energy and the transport calculations. The structures are optimized by relaxing the position of the anchoring group and the pyramids while keeping the rest of the Au atoms fixed in the bulk positions. Before calculating the transmission function, the DFT eigenstates are transformed into a set of localized Wannier-like basis functions [14]. This transformation makes it possible to partition the system into a central region (containing the contact region of the junction) and a left and right lead (bulk gold). In this way, the Landauer–Büttiker conductance, G, can be calculated from the Green's function of the central region, G_C, according to the formula [15, 16]

$$G = G_0 \, \mathrm{Tr}[G_C \Gamma_L G_C^\dagger \Gamma_R]|_{\varepsilon=\varepsilon_F}, \qquad (1)$$

where the trace runs over all localized basis functions in the central region and $G_0 = 2e^2/h$ is the conductance quantum. The central region Green's function is calculated from

$$G_C(\varepsilon) = ((\varepsilon + i0^+)S_C - H_C^{KS} - \Sigma_L(\varepsilon) - \Sigma_R(\varepsilon))^{-1}, \quad (2)$$

where S_C and H_C^{KS} are the overlap matrix and Kohn–Sham Hamiltonian matrix of the central region in the localized basis, and $\Sigma_{L/R}$ are lead self-energies. The coupling strengths are given by $\Gamma_{L/R} = i(\Sigma_{L/R} - \Sigma_{L/R}^\dagger)$. More details on the Wannier transport scheme may be found in [17].

3. Results

To gain insight into the possible structures of an Au–S/NH$_2$–Au contact, we have made successive relaxations of the system as the distances between the outermost surface layers is varied, thereby simulating the contact formation in a break junction experiment. When increasing the distance between the two Au(111) surfaces, all atomic distances between them have been proportionally increased and subsequently relaxed. In the
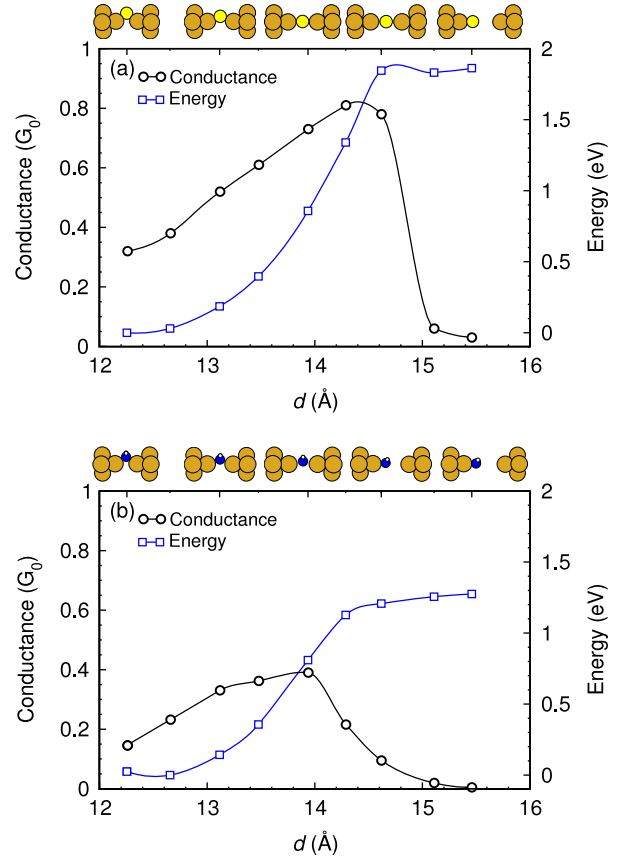
Figure 1. Conductance (circles) and total energy (squares) for (a) Au–S–Au and (b) Au–NH$_2$–Au nanojunctions in the symmetric top–top configuration as a function of distance between the outermost Au(111) surfaces. The breaking forces are approximately 1.8 and 1.0 eV Å^{-1}, respectively. The zero points of the energy have been chosen arbitrarily. Notice that for both systems the conductance increases as the contact is pulled apart due to the linearization of the contact geometry.

following we concentrate on two different structures for the gold contacts: (i) two opposing pyramids and (ii) a pyramid opposing a pyramid with the tip atom removed, with geometries as shown schematically in figures 1 and 4, respectively. For contact (i) both S and NH$_2$ bind symmetrically to the tip atoms of the two pyramids. We refer to these as (symmetric) top–top configurations. For contact (ii), S adopts the site of the removed Au tip atom, thus forming a top–hollow configuration. However, NH$_2$ forms a bridge between the pyramid tip atom and one of the three gold atoms forming the pyramid base (the asymmetric top–top configuration). We note that the sulfur top–top and top–hollow configurations correspond to the configurations proposed in [18]. We also mention that molecular dynamics simulations of sulfur-contaminated gold contacts frequently result in Au–S–Au contacts similar to the ones studied here [19].

Consider first the sulfur top–top structure, shown in figure 1(a). For short distances between the Au(111) surfaces, the S atom is situated at the side of the contact bridging the two Au tip atoms. As the contact is pulled apart, the sulfur atom moves into the contact, resulting in a linear contact configuration. Interestingly, the conductance increases from
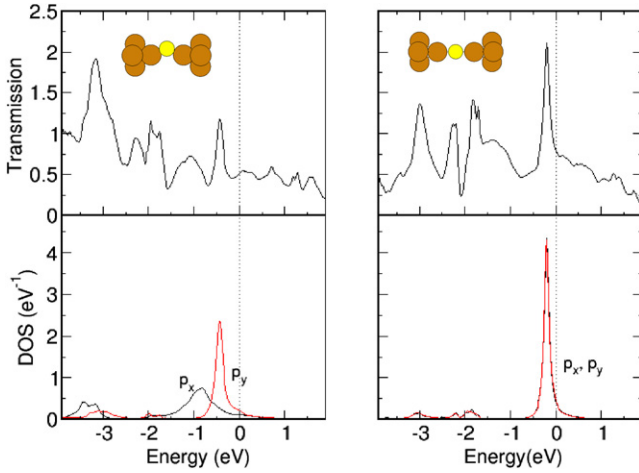
Figure 2. Total transmission (upper panels) and projected density of states (PDOS) for the p-orbitals perpendicular to the contact axis (lower panels) for a contracted (left) and stretched (right) Au–S–Au contact. The center of both the p-orbitals moves closer to the Fermi level as the contact is elongated. The p_x-orbital (pointing towards the sulfur atom) is completely quenched for the contracted contact due to the coupling to the gold s-band. Both effects result in the observed increase in the conductance as the contact is stretched.
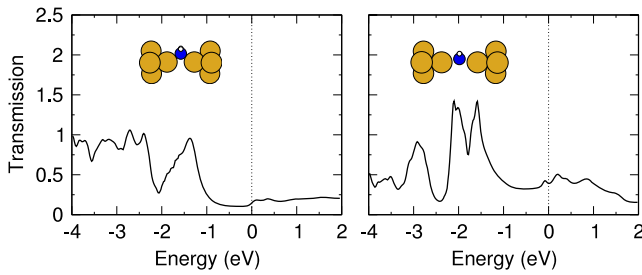

Figure 3. Total transmission for a contracted (left) and stretched (right) Au–NH$_2$–Au contact. Notice that the transmission function varies little around the Fermi level as compared to the transmission function of the Au–S–Au contact shown in figure 2.

Figure 4. Conductance (circles) and total energy (squares) for (a) Au–S–Au and (b) Au–NH$_2$–Au nanojunctions in the top–hollow and asymmetric top–top configurations, respectively, as a function of distance between the outermost Au(111) surfaces. The breaking forces are approximately 1.0 and 0.9 eV Å^{-1}, respectively.

$0.3G_0$ to $0.8G_0$ as the contact is pulled apart, demonstrating how small changes in the local atomic structure of the contact can lead to significant changes in the conductance of the junction. In general, such behavior is characteristic of the phase-coherent transport regime and is a direct manifestation of the wave nature of the charge carriers.

The observed increase in conductance as the contact is stretched is mainly due to the sulfur p_x-orbital (the x axis is vertical on all plots of the structure). To show this, we compare in figure 2 the transmission function and the projected density of states (PDOS) for the p_x-and p_y-orbitals at two different elongations of the contact. The peak in the transmission function just below the Fermi level is clearly correlated to the PDOS of the p_x-and p_y-orbitals. As the contact is stretched, the peak grows in intensity by a factor of two and is shifted closer to E_F. The increase in intensity is due to the opening of the p_x channel. For the contracted configuration the PDOS of p_x is broadened and shifted downwards by the coupling to the gold s-band. In the linear configuration, this coupling is prohibited by symmetry and p_x and p_y are degenerate.
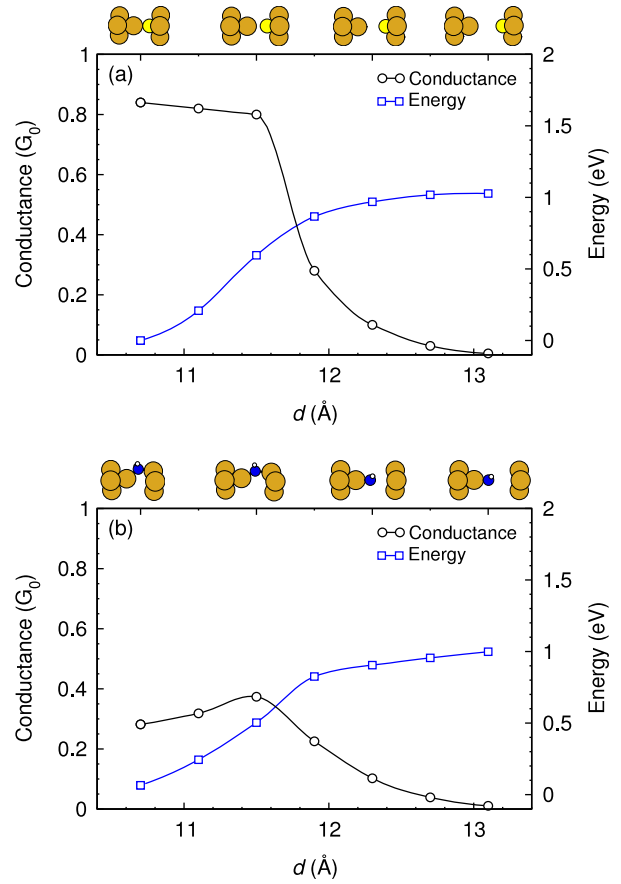
Besides the contribution from the p_x- and p_y-orbitals, the total transmission also includes a background contribution from the p_z-orbital pointing in the transport direction. However, this background contribution stays almost constant when the system is elongated. More generally, the sharp peaks in the transmission function very close to E_F makes the conductance sensitive to changes in the surrounding potential.

Next, we consider the symmetric NH$_2$ top–top structure shown in figure 1(b). The structural change upon pulling is rather similar to the sulfur junction. However, the conductance is somewhat lower and increases from about $0.2G_0$ to $0.4G_0$. We note that the drop in conductance when the contact breaks is less abrupt than for the sulfur junction. This is due to the weakness of the Au–NH$_2$ bond as compared to the Au–S bond, which implies that the gold pyramids retract less when the NH$_2$ junction breaks. More generally, the continuous drop in conductance upon rupture is an artifact of the finite size of the supercell which prohibits a large retraction of the contact when it breaks. The transmission functions of the NH$_2$ junction for two different elongations are shown in figure 3. In comparison with the sulfur junction, the transmission functions of the amine junction show little variation around E_F. Thus small changes in the nearby electron potential due

to changes in the gold contacts should have little effect on the conductance.

In the Au–S–Au top–hollow configuration, the sulfur atom occupies the site of the removed tip atom of one of the two pyramids, as shown in the schematics of figure 4(a). When the junction is pulled, no major rearrangements of the atoms occur and the conductance stays rather constant around $0.8G_0$ until the contact breaks. We notice that the conductance trace of the top–hollow configuration is distinctly different from the trace of the top–top configuration in figure 1(a). In particular, the conductance does not increase upon pulling but stays almost constant until the breaking point.

The calculated conductance trace of the asymmetric NH_2 top–top configuration (the same Au contact geometry as for the sulfur top–hollow) is shown in figure 4(b). The conductance increases from $0.3G_0$ to $0.4G_0$ as the junction is pulled and is quite similar to the symmetric NH_2 top–top configuration of figure 1(b). The reason for the similarity with the symmetric top–top configuration is that in both cases NH_2 binds to a single gold atom on each side of the contact. This is due to the fact that the hydrogen atoms occupy two of the four available sp^3 hybrid sites, which leaves only two unoccupied orbitals for the gold bonds. Obviously this is in contrast to sulfur, which can form bonds to four gold atoms as in the top–hollow configuration of figure 4(a).

4. Summary

With the aim of identifying and comparing the intrinsic properties of thiol and amine anchoring groups in relation to molecular electronics, we have presented DFT calculations of the structure and conductance of Au–S–Au and Au–NH_2–Au nanojunctions. The main result is that the structural selectivity of the amine group leads to small junction to junction fluctuations in the conductance traces of the Au–NH_2–Au junctions, whereas the larger variability in sulphur–gold bonding geometries leads to significantly different Au–S–Au conductance traces depending on the atomic structure of the gold contacts. Thus, the intrinsic transport properties of the amine group are more well defined than those of the thiol. This supports the experimental finding that amine-bonded molecules are easier to characterize in terms of conductivity than thiol-bonded molecules. The similarity of the conductance traces of the Au–NH_2–Au junctions should lead to a peak around $0.4G_0$ in a conductance histogram. On the other hand, the structural sensitivity of Au–S–Au junctions may produce a histogram without clear features. However, it

should be possible to identify the sulfur top–top structure from its characteristically rising conductance trace.

References

[1] Ulrich J, Esrail D, Pontius W, Venkataraman L, Millar D and Doerrer L H 2006 *J. Phys. Chem.* B **110** 2462
[2] Reed M A, Zhou C, Muller C J, Burgin T P and Tour J M 1997 *Science* **278** 252
[3] Xiao X, Xu B and Tao N J 2004 *Nano Lett.* **4** 267
[4] Tsutsui M, Teramae Y, Kurokawa S and Sakai A 2006 *Appl. Phys. Lett.* **89** 163111
[5] Ghosh S, Halimun H, Mahapatro A K, Choi J, Lodha S and Janes D 2005 *Appl. Phys. Lett.* **87** 233509
[6] Quek S Y, Venkataraman L, Choi H J, Louie S G, Hybertsen M S and Neaton J B 2007 *Nano Lett.* **7** 3477
[7] Yanson A I, Rubio Bollinger G, van der Brom H E, Agrait N and Ruitenbeek J M 1998 *Nature* **395** 783
[8] Rubio-Bollinger G, Bahn S R, Agraït N, Jacobsen K W and Vieira S 2001 *Phys. Rev. Lett.* **87** 026101
[9] Djukic D, Thygesen K S, Untiedt C, Smit R H M, Jacobsen K W and van Ruitenbeek J M 2005 *Phys. Rev.* B **71** 161402(R)
[10] Garca-Surez V M, Rocha A R, Bailey S W, Lambert C J, Sanvito S and Ferrer J 2005 *Phys. Rev.* B **72** 045437
[11] Ke S-H, Baranger H U and Yang W 2005 *J. Chem. Phys.* **122** 74704
[12] Mowbray D J, Jones G and Thygesen K S 2008 *J. Chem. Phys.* **128** 111103
[13] Bahn S R and Jacobsen K W 2002 *Comput. Sci. Eng.* **4** 56 (The Dacapo code can be downloaded at http://www.camd.dtu.dk/software)
[14] Thygesen K S, Hansen L B and Jacobsen K W 2005 *Phys. Rev. Lett.* **94** 026405
[15] Meir Y and Wingreen N S 1992 *Phys. Rev. Lett.* **68** 2512
[16] Thygesen K S 2006 *Phys. Rev.* B **73** 035309
[17] Thygesen K S and Jacobsen K W 2005 *Chem. Phys.* **319** 111
[18] Li X, He J, Hihath J, Xu B, Lindsay S M and Tao N 2006 *J. Am. Chem. Soc.* **128** 2135
[19] Anglada E, Torres J A, Yndurain F and Soler J M 2007 *Phys. Rev. Lett.* **98** 096102
[20] Perdew J P, Chevary J A, Vosko S H, Jackson K A, Pederson M R, Singh D J and Fiolhais C 1992 *Phys. Rev.* B **46** 6671